

**FORMATION TIMESCALES OF WARK-LOVERING RIMS AROUND CALCIUM-ALUMINUM RICH INCLUSIONS.** P. Mane<sup>1</sup>, M. Bose<sup>2</sup>, C. Defouilloy<sup>3</sup>, N. T. Kita<sup>3</sup>, G. J. MacPherson<sup>4</sup>, and M. Wadhwa<sup>1</sup>, <sup>1</sup>School of Earth and Space Exploration, Arizona State University, Tempe, AZ 85287. (Email: [Prajakta.Mane@asu.edu](mailto:Prajakta.Mane@asu.edu)). <sup>2</sup>School of Molecular Sciences, Arizona State University, Tempe, AZ 85287. <sup>3</sup>WiscSIMS, Department of Geoscience, University of Wisconsin-Madison, Madison, WI 53706. <sup>4</sup>US National Museum of Natural History, Smithsonian Institution, Washington, D.C., 20560.

**Introduction:** Calcium-Aluminum-rich Inclusions (CAIs) are thought to be the first solids to form in the early Solar System [1-4]. These inclusions are surrounded by mono- and bi-mineralic rim sequences, called the “Wark-Lovering” (WL) rims [5], which are made of Ca- and Al-rich refractory minerals, similar to their parent CAIs. In some CAIs, the rim sequence is heterogeneous in its  $\Delta^{17}\text{O}$  composition, suggesting that these mineral layers sampled spatially or temporally distinct oxygen reservoirs [6-9]. The  $^{26}\text{Al}$ - $^{26}\text{Mg}$  chronometry shows a range of relative ages from 0 to ~2 Ma between the formation of the CAIs and their WL rims [10-16]. In order to better understand the formation timescales and formation mechanism of WL rims, we analyzed and report here the oxygen isotopic compositions, and additional Al-Mg isotopic compositions of the WL rims of two CAIs from the CV3 chondrite Northwest Africa (NWA) 8323 for which we previously showed a ~2 My time difference (based on Al-Mg isotopes) between the CAIs and their rim formation [14].

**Analytical Methods:** Characterization of the CAIs and their WL rim sequences was done using a JEOL JXA-8530F electron microprobe at Arizona State University (ASU) and a FEI NOVA NanoSEM 600 field-emission gun scanning electron microscope at the Smithsonian Institution. Magnesium and oxygen isotope analyses were conducted using secondary ion mass spectrometry (SIMS), specifically a NanoSIMS 50L at ASU and the WiscSIMS IMS 1280, respectively, with analytical conditions similar to those described previously [14, 17]. To assess the alteration effects in the CAIs and the rim minerals, major and trace elemental abundances were measured using the JEOL JXA-8530F electron microprobe and the Cameca IMS 6f SIMS, respectively, at ASU.

**Petrography, Major and Trace Element Analyses:** NWA 8323 is an oxidized subgroup CV3 chondrite that shows a low shock grade and minimal weathering effects [18]. Both CAIs (CAI-1 and CAI-2) are coarse-grained type B inclusions containing melilite, spinel, Ti-rich pyroxene, and anorthite. The WL rim sequence in CAI-1 consists of olivine, spinel, pyroxene and anorthite (Fig. 1); in some regions the rim sequence shows Fe-rich spinels and glass. The CAI-2 inclusion has a partially formed rim sequence com-

prised of a spinel layer in one portion of the inclusion, whereas the other side of the inclusion shows a sequence of spinel, pyroxene and anorthite and olivine.

The WL rims in most CAIs contain fine-grained anorthite as a secondary alteration product, replacing the melilite layer [19]. However, the interior and the rim layer anorthites in these two inclusions are unusual, as they show coarse-grained textures, indicating crystallization from melt. There are some regions of the WL rims in these two CAIs that show presence of nepheline and alteration textures, which are likely produced by parent body processes. However, most coarse-grained regions show absence of elevated Na and Fe in the anorthites, suggesting minimal secondary alteration. Moreover, the Ba/Sr versus Eu/Sr ratios in these two CAIs suggest that Sr has not been mobilized during secondary alteration.

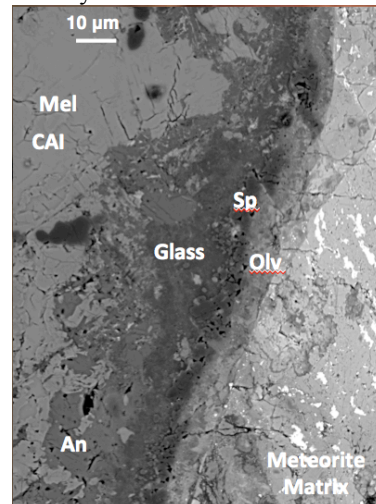


Figure 1: Back Scattered Electron (BSE) image of CAI-1, its WL rim, and the surrounding matrix. The image shows melilite (Mel) in the CAI interior; the phases in the WL rim shown here are olivine (Olv), spinel (Sp), anorthite (An) and glass.

**$^{26}\text{Al}$ - $^{26}\text{Mg}$  Systematics:** The Mg isotopic analyses of rims were conducted on the coarse-grained regions of the rims that are thought to be unaffected by secondary alteration. The preliminary results were reported earlier [14]. The interior of the CAI-1 shows evidence for a  $^{26}\text{Al}/^{27}\text{Al}$  ratio of  $(5.2 \pm 0.6) \times 10^{-5}$ , with initial  $(\delta^{26}\text{Mg}^*)_0$  of  $1.7 \pm 4.7\%$  (MSWD = 2.9). In the WL rim for CAI-1, the  $^{26}\text{Al}/^{27}\text{Al}$  ratio was inferred to be  $(6.2 \pm 3.2) \times 10^{-6}$ , with initial  $(\delta^{26}\text{Mg}^*)_0$  of  $3.4 \pm 2.7\%$  (MSWD = 0.5). The relative time between for-

mation of CAI-1 interior and its WL rim is  $2.2^{+0.7}_{-0.4}$  Ma. The interior of the CAI-2 shows evidence for a  $^{26}\text{Al}/^{27}\text{Al}$  ratio of  $(5.2 \pm 0.4) \times 10^{-5}$ , with  $(\delta^{26}\text{Mg}^*)_0$  of  $5.8 \pm 3.9\%$  (MSWD = 2.1). In the WL rim for CAI-2, the  $^{26}\text{Al}/^{27}\text{Al}$  ratio was inferred to be  $(4.5 \pm 3.4) \times 10^{-6}$ , with  $(\delta^{26}\text{Mg}^*)_0$  of  $4.4 \pm 3.1\%$  (MSWD = 1.0). The relative time between formation of CAI-2 interior and its WL rim is  $2.5^{+1.5}_{-0.6}$  Ma.

**O Isotope Systematics:** In terms of  $\Delta^{17}\text{O}$ , phases in the two CAIs range from the CAI end-member ( $\Delta^{17}\text{O} = -25\%$ ) up to the terrestrial value ( $\Delta^{17}\text{O} = 0\%$ ) (Fig. 2). The interior spinels show  $\Delta^{17}\text{O}$  values of  $-24 \pm 2\%$  (2SD). The interior pyroxenes also show a restricted range in  $\Delta^{17}\text{O}$  of  $-24.2 \pm 1.6\%$  to  $-20 \pm 1\%$ . The interior melilites show  $\Delta^{17}\text{O}$  values that are close to terrestrial (ranging from  $-9 \pm 2\%$  to  $-1 \pm 2\%$ ). The interior anorthites show a range in  $\Delta^{17}\text{O}$  of  $-11 \pm 2\%$  to  $-1 \pm 2\%$ . The WL rim spinels show a restricted range in  $\Delta^{17}\text{O}$  of  $-19 \pm 2\%$  to  $-22 \pm 2\%$ . The rim pyroxenes show  $\Delta^{17}\text{O}$  values ranging from  $-24 \pm 2\%$  to  $-8 \pm 2\%$ . The rim anorthites show  $\Delta^{17}\text{O}$  values in the range of  $-4 \pm 2\%$  to  $0 \pm 2\%$ .

**Discussion:** The texture, mineralogy and chemistry of the two CAIs and their associated WL rims analyzed here indicate formation in a complex and dynamic setting. The anorthite layer in the WL rim in each of these two CAIs is coarse-grained, and appears to have crystallized from a melt, unlike the anorthite in most previously described rim sequences. The O isotopes in anorthites in the rims and the interiors are partially exchanged whereas both interior and rim spinels are  $^{16}\text{O}$ -rich, suggesting that both interior and rim anorthites may have started with a  $^{16}\text{O}$ -rich composition and later exchanged. It seems likely that these texturally atypical rims in the two CAIs studied here were produced by melting events in the solar nebula and have not been significantly altered by parent body processes. This is supported by the fact that the rim and interior phases in these two inclusions define two distinct Al-Mg isochrons, recording two separate events, with the later likely associated with the melting event resulting in the formation of the phases in the rim. The time difference of  $\sim 2$  Ma between the interiors of these two CAIs and their rims coincides with the majority of chondrule formation ages, suggesting that these rims may have formed in flash-heating events similar to those that produced the majority of chondrules in the early Solar System. This time difference additionally implies that CAIs remained as free floating objects for  $\sim 2$  Ma before accreting into planetesimals.

**References:** [1] Amelin Y. et al. (2002) *Science*, 297, 1678-1683. [2] Amelin Y. et al. (2009) *GCA*, 73, 5212-5223. [3] Bouvier A. and Wadhwa M. (2010) *Nature Geosci.*, 3,

637-641. [4] Connelly J. N. et al. (2012) *Science*, 338, 651-655. [5] Wark D. A. & Lovering J. F. (1977) *LPSC IIX*, 95-112. [6] Hirai K. et al. (2002) *LPSC XXXIII*, Abstract #1419. [7] Yoshitake M. et al. (2002) *LPSC XXXIII*, Abstract #1502. [8] Ito M. & Messenger S. (2010) *MAPS*, 45, 583-595. [9] Simon J. I. et al. (2011) *Science* 331, 1175-1178. [10] Co-sarinsky M. et al. (2005) *LPSC XXXVI*, Abstract #2105. [11] Taylor D. J. et al (2005) *LPSC XXXVI*, Abstract #2030. [12] Simon J. I. et al. (2005) *EPSL*, 238, 272-283. [13] Kawasaki N. et al. (2015) *LPI Contributions* 1856, 5028. [14] Mane P. et al. (2015) *LPSC XLVI*, Abstract #2898. [15] Mane P. et al. (2015) *LPI Contributions* 1856, 5327 [16] Matzel J. et al. (2015) *LPI Contributions* 1856, 5372. [17] Ushikubo T. et al. (2011) *Workshop on Formation of the First Solids in the Solar System*, #9086. [18] *Met. Bull.* #103 (2014) in prep. [19] MacPherson G. J. (2014) *Treatise on Geochemistry* 2: 201-246.

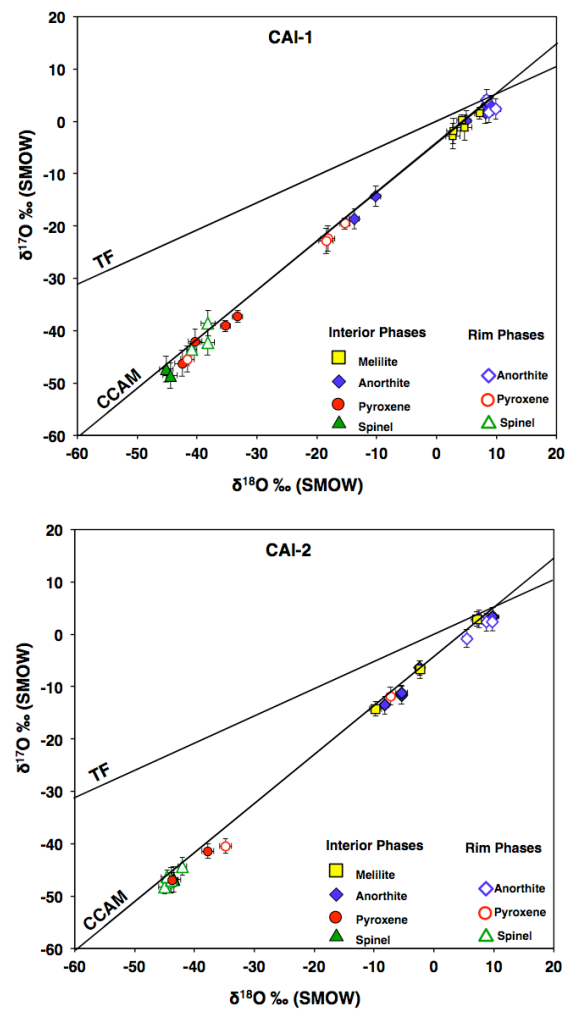


Figure 2: Oxygen isotope compositions of interior and rim phases of CAI-1 and CAI-2. TF: Terrestrial Fractionation line; CCAM: Carbonaceous Chondrite Anhydrous Minerals line.